Letter

Strong correlations in lossy one-dimensional quantum gases: From the quantum Zeno effect to the generalized Gibbs ensemble

Davide Rossini,[1,2] Alexis Ghermaoui,[3] Manel Bosch Aguilera,[3,*] Rémy Vatré,[3] Raphaël Bouganne,[3] Jérôme Beugnon,[3] Fabrice Gerbier,[3] and Leonardo Mazza[2,†]

[1]*Dipartimento di Fisica dell'Università di Pisa and INFN, Largo Pontecorvo 3, 56127 Pisa, Italy*

[2]*Université Paris-Saclay, CNRS, LPTMS, 91405 Orsay, France*

[3]*Laboratoire Kastler Brossel, Collège de France, CNRS, ENS-PSL Research University, Sorbonne Université, 11 Place Marcelin Berthelot, 75005 Paris, France*

(Received 9 November 2020; accepted 10 June 2021; published 24 June 2021)

We consider strong two-body losses in bosonic gases trapped in one-dimensional optical lattices. We exploit the separation of timescales typical of a system in the many-body quantum Zeno regime to establish a connection with the theory of the time-dependent generalized Gibbs ensemble. Our main result is a simple set of rate equations that capture the simultaneous action of coherent evolution and two-body losses. This treatment gives an accurate description of the dynamics of a gas prepared in a Mott insulating state and shows that its long-time behavior deviates significantly from mean-field analyses. The possibility of observing our predictions in an experiment with ^{174}Yb in a metastable state is also discussed.

DOI: 10.1103/PhysRevA.103.L060201

Introduction. Dissipation, noise, and losses are ubiquitous in experiments with quantum systems. Although they are typically associated with decoherence [1], they can also induce interesting phenomena. An iconic example is the quantum Zeno effect, according to which the lifetime of an unstable quantum system can dramatically increase if it is repeatedly (or even continuously) observed [2–4]. The same effect also arises for a quantum system dissipatively coupled to an external environment, since this situation can always be interpreted as a generalized (unread) measurement [5–7].

While earlier studies focused on simple quantum systems, there is increasing interest and progress in out-of-equilibrium many-body quantum physics. This field is still in its infancy, but several flexible platforms are now available for experimental studies, e.g., trapped ions [8], cavity polaritons [9], photons in nonlinear media [10], and ultracold atomic or molecular gases [11–19]. A major goal is not only to understand quantitatively the effect of decoherence, but also to harness dissipative phenomena to engineer specific quantum states, or even to enhance quantum coherence and correlations [20–26].

Among all sources of dissipation, n-body losses ($n \geqslant 2$) are particularly interesting because they reduce to an n-body hard-core constraint [26–29]. This effect was demonstrated experimentally with a bosonic one-dimensional gas of molecules subject to two-body losses ($n = 2$) [30]. Strong losses lead to an emergent behavior of the molecules as fermionized (hard-core) bosons [31], evidenced by the counterintuitive *increase* of the lifetime of the gas when two-body losses become stronger. This pioneering experiment demonstrates a paradigmatic instance of the many-body quantum Zeno effect, where the losses are interpreted as fast and unread measurements. This phenomenon has been probed further in ultracold atomic gases with native [32] or photoassociative [17] two-body losses, in multicomponent fermionic mixtures [33–35], or bosonic systems with three-body losses [36].

In this Letter, we study the dynamics of bosonic gases with two-body losses beyond mean field. We find evidence for an out-of-equilibrium correlated regime at long times caused by the interplay between coherent dynamics and losses. We identify two main experimental signatures as hallmarks of this regime: (i) the decay of the bosonic population as $t^{-1/2}$ [instead of $1/t$ for the uncorrelated hard-core boson (HCB) gas [31]], and (ii) the emergence of peaks centered around $k = 0$ and π in the momentum distribution. To derive these results, we establish and exploit a connection between the many-body quantum Zeno effect and generalized Gibbs ensembles (GGEs) describing the pseudothermalization of an isolated quantum system [37–45]. This connection allows us to derive physically transparent rate equations which give predictions in excellent agreement with numerical exact simulations.

The problem. We consider a one-dimensional bosonic gas trapped in an optical lattice and subject to on-site two-body losses. The unitary dynamics is governed by a single-band Bose-Hubbard Hamiltonian $H_0 = -J\sum_j (b_j^\dagger b_{j+1} + \text{H.c.}) + (U/2)\sum_j b_j^{\dagger 2} b_j^2$, where $b_j^{(\dagger)}$ are bosonic annihilation (creation) operators satisfying canonical commutation relations, while J is the hopping amplitude and U the (repulsive) real part of the on-site interaction strength. The full dynamics is described by a Lindblad master equation for the density matrix $\rho(t)$ [30,31,46]:

$$\frac{d}{dt}\rho = \mathcal{L}[\rho] = -\frac{i}{\hbar}[H_0, \rho] + \mathcal{D}[\rho]; \tag{1a}$$

$$\mathcal{D}[\rho] = \sum_j L_j \rho L_j^\dagger - \frac{1}{2}\{L_j^\dagger L_j, \rho\}. \tag{1b}$$

*Present address: Department of Physics, University of Basel, Klingelbergstrasse 82, 4056 Basel, Switzerland.

†leonardo.mazza@universite-paris-saclay.fr

The first term in the right-hand side of (1a) describes the unitary evolution, and the second term $\mathcal{D}[\rho]$ the dissipative evolution driven by *jump operators* L_j for each site j. The jump operators describing two-body losses are $L_j = \sqrt{\gamma_{2B}/2}\, b_j^2$, where $-\hbar\gamma_{2B}/2$ is the imaginary part of the interaction strength [47]. The ratio γ_{2B}/U is typically fixed by the atomic or molecular properties; in contrast, the ratio γ_{2B}/J is tunable by several orders of magnitude.

We consider a system that is initially in an atomic-limit Mott insulator ($J = 0$) with one atom per site. The initial state ρ_0 is stable under two-body losses for $J = 0$ (indeed $\mathcal{L}[\rho_0] = 0$). At $t = 0$, the lattice depth is lowered ($J > 0$). Atoms can tunnel to neighboring sites and reach unstable configurations with doubly occupied sites. Our goal is to characterize the dissipative dynamics, focusing on readily measurable observables such as the total number of particles $N(t) = \mathrm{Tr}[\sum_j b_j^\dagger b_j\, \rho(t)]$.

Many-body quantum Zeno effect. We focus on the quantum-Zeno limit of strong dissipation $\hbar\gamma_{2B} \gg J$. Roughly speaking, all Fock states with at least one doubly—or higher—occupied site decay almost immediately on a timescale $\sim\gamma_{2B}^{-1}$. This decay thus occurs before any substantial coherent dynamics can take place. The subspace of Fock states with at most one boson per lattice site is quasistationary and the long-time dynamics takes place in this space of fermionized HCB [4]. This kinematic constraint results solely from the strong losses, and already shows that they induce nontrivial correlations.

Using the separation of timescales $\gamma_{2B}^{-1} \ll \hbar/J$, Ref. [31] proposes an effective Lindblad master equation $\frac{d}{dt}\rho = \mathcal{L}'[\rho]$ that describes the long-time dynamics in the HCB subspace. The effective Hamiltonian is $H' = -J\sum_j(\beta_j^\dagger\beta_{j+1} + \mathrm{H.c.})$ and corresponds to a tight-binding model of HCB annihilated by the operators β_j. The effective jump operators take the form of inelastic nearest-neighbor interactions $L'_j = \sqrt{\Gamma_{\mathrm{eff}}}\beta_j(\beta_{j-1} + \beta_{j+1})$, with

$$\Gamma_{\mathrm{eff}} = \frac{8}{1 + \left(\frac{2U}{\hbar\gamma_{2B}}\right)^2}\frac{J^2}{\hbar^2\gamma_{2B}}. \tag{2}$$

The effective dissipative dynamics is governed by a novel timescale $\Gamma_{\mathrm{eff}}^{-1} \gg \hbar/J \gg \gamma_{2B}^{-1}$. These inequalities and the scaling $\Gamma_{\mathrm{eff}}^{-1} \propto J^2/\gamma_{2B}$ are typical of the quantum Zeno regime.

The master equation implies a decay law for the mean atom number $\frac{d\bar{N}}{dt} = -2\sum_j\langle L_j'^\dagger L'_j\rangle$. The correlator on the right-hand side involves inelastic nearest-neighbors interactions $\propto\langle n_j n_{j\pm1}\rangle$ and phase-sensitive density-dependent tunneling $\propto\langle\beta_{j\pm1}^\dagger n_j\beta_{j\mp1}\rangle$, where $n_j = \beta_j^\dagger\beta_j$ is the HCB density. Assuming no correlations between sites, i.e., $\langle L_j'^\dagger L'_j\rangle \approx 2\langle n_j\rangle^2$, Ref. [31] derived the mean-field solution,

$$N(t)/L = (1 + 4\Gamma_{\mathrm{eff}}t)^{-1}, \tag{3}$$

with L the system length. We note that experimental and numerical data are typically analyzed using heuristic modifications of this equation [30,31,35].

In Fig. 1 we compare Eq. (3) with a numerical solution of the HCB model $\frac{d}{dt}\rho = \mathcal{L}'[\rho]$ obtained with state-of-the-art techniques based on quantum trajectories [48] for sizes up to $L = 14$. These simulations do not rely on physical approximations and serve here as a benchmark. Unsurprisingly, the mean-field solution agrees with the numerics only at short times because the initial state is uncorrelated. Increasingly strong deviations appear at long times, indicating the buildup of correlations that the mean-field model fails to capture.

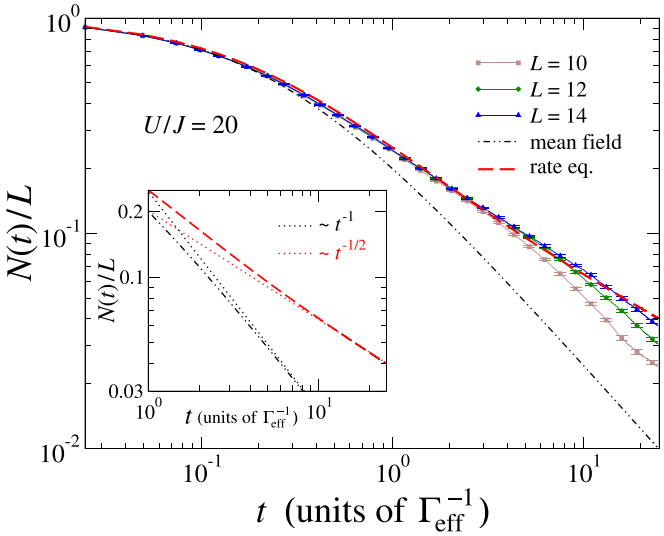

FIG. 1. Time evolution of the number of atoms according to the rate equations (5) for the initial state ρ_0 (dashed red line). We take $U/J = 20$ and $U/(\hbar\gamma_{2B}) = 1.33$ as in ^{174}Yb. Our result is benchmarked with simulations based on quantum trajectories for $L = 10$, 12, and 14 (each point is averaged over 10^4 trajectories and the associated statistical error bars are shown only for some points to increase readability). The dot-dashed black line represents the mean-field solution $N(t)/L$ in Eq. (3). The inset highlights the different long-time decay as t^{-1} for the mean-field solution and as $t^{-1/2}$ for the rate equation.

Rate equations. We now describe our analytical approach to the correlated dissipative dynamics. We interpret the dissipative dynamics as periods of unitary evolution interrupted by quantum jumps where a loss event takes place [48]. Two consecutive loss events are spaced by a time interval $\sim\Gamma_{\mathrm{eff}}^{-1}$. Since the typical timescale of the unitary dynamics of H' is $\hbar/J$, we conclude that according to the inequality $\hbar/J \ll \Gamma_{\mathrm{eff}}^{-1}$, the unitary dynamics taking place in between is *long*.

This dynamics is most easily analyzed after a Jordan-Wigner transformation [49] mapping the HCB to free fermions. Considering periodic boundary conditions, H' then becomes a free fermionic Hamiltonian $H' = \sum_k \varepsilon(k)c_k^\dagger c_k$, with k the quasimomentum, $c_k^{(\dagger)}$ canonical fermionic operators, and $\varepsilon(k) = -2J\cos(k)$.

The theory of generalized thermalization in closed quantum systems allows us to describe the state reached after a long unitary evolution of H' as a pseudothermal state σ taking all possible conservation laws into account—a GGE [38–41]. This pseudothermal state σ is Gaussian in momentum space, thus completely characterized by its correlation matrix $g_{kq} = \mathrm{Tr}[c_k^\dagger c_q\,\sigma]$. The latter is diagonal for a noninteracting and translationally invariant Fermi gas [50],

$$g_{kq} = \delta_{kq}n_k, \tag{4}$$

where δ_{kq} is the Kronecker delta. We now assume that losses are so rare that the system has enough time in between two

loss events to reach a Gaussian generalized-thermal state obeying Eq. (4). A complete characterization of the dynamics then only requires the knowledge of the occupation number of the different fermionic momenta $n_k(t) = \mathrm{Tr}[c_k^\dagger c_k \rho(t)]$.

We propose to characterize completely the loss dynamics of $N(t)$ by assuming that (i) at every time t the state $\rho(t)$ is Gaussian, and that (ii) it always satisfies momentum factorization (4). Starting from the Lindblad master equation (in the fermionic formulation) and using the aforementioned properties (i) and (ii), we obtain after some algebra the following rate equations [51]:

$$\frac{d}{dt} n_k(t) = -\frac{4\Gamma_{\mathrm{eff}}}{L} \sum_q [\sin(k) - \sin(q)]^2 n_q(t)\, n_k(t). \qquad (5)$$

These equations constitute the main result of this Letter.

Decay of the total number of atoms. The equations (5) are easily solved numerically. Provided time is properly rescaled in units of $\Gamma_{\mathrm{eff}}^{-1}$, we expect that the curves $n_k(t)$ collapse onto a universal function $f_k(x)$ with $x = \Gamma_{\mathrm{eff}} t$; similarly, $N(t)$ will collapse onto a function $f(x)$. The initial state has unit occupation for each momentum, $n_k(0) = 1$. In the fermionic representation, it corresponds to a band insulator with the lowest Bloch band entirely filled.

We plot in Fig. 1 the density $N(t)/L$ as a function of time for $L = 100$ (indistinguishable from the thermodynamic limit, not shown). We observe an excellent agreement between the prediction of the rate equation and the numerical simulations for all considered times bearing finite size effects. We thus conclude that the rate equations (5), despite their simplicity, indeed capture the behavior of a complex, interacting and dissipative system. Moreover, for a negligible computational cost, they give access to the thermodynamic-limit behavior.

Unlike the mean-field solution, which predicts the scaling $N_0(t) \propto t^{-1}$ at long times, the rate equations (5) predict that $N(t)$ decays to zero as $t^{-1/2}$. This result is highlighted in the inset of Fig. 1 and can be analytically proven [51]. This algebraic decay is the hallmark of the correlations that build up after dissipation is enabled.

Momentum distribution function. The rate equations (5) provide direct access to the *fermionic* occupation number $n_k(t)$. In the Supplemental Material [51], we show that the fermionic momentum distribution is well approximated in the long-time limit $t > \Gamma_{\mathrm{eff}}^{-1}$ by

$$n_k(t) \approx \frac{1}{(8\pi\Gamma_{\mathrm{eff}} t)^{1/4}} e^{-\sin^2(k)\,(8\Gamma_{\mathrm{eff}} t/\pi)^{1/2}}. \qquad (6)$$

In Fig. 2 (left), we plot $n_k(t)$ for different times, from $t = 0$ to $t \sim 2.5\Gamma_{\mathrm{eff}}^{-1}$, and find excellent agreement with the simulations [51]. Although at initial times the population is uniformly spread among the different momenta, a double-peaked distribution emerges for long times, with maxima at $k = 0, \pi$. The interplay between two-body losses and coherent free-fermion dynamics has thus created a nonequilibrium fermionic gas where the notion of Fermi sea is completely lost.

Standard time-of-flight measurements give instead access to the *bosonic* momentum distribution function $\langle b_k^\dagger b_k \rangle_t$, where $b_k = L^{-1/2} \sum_j e^{ikj} b_j$ is a canonical bosonic operator. The link between $\langle b_k^\dagger b_k \rangle_t = \mathrm{Tr}[b_k^\dagger b_k\, \rho(t)]$ and $n_k(t)$ is known explicitly and we use the approach presented in Ref. [52] to compute

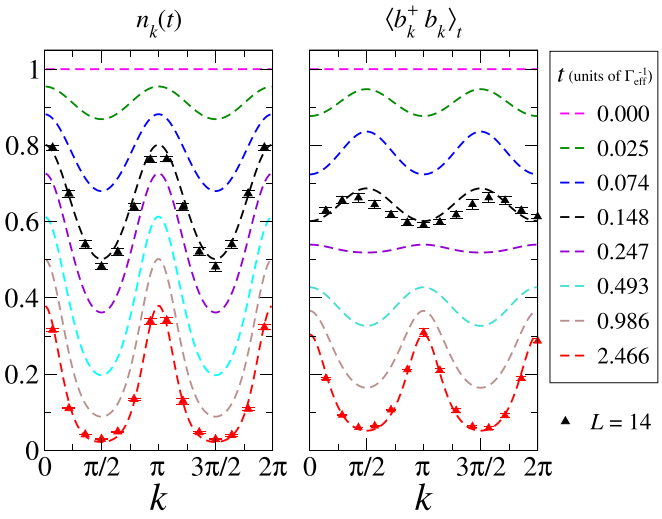

FIG. 2. Fermionic (left) and bosonic (right) quasimomentum distributions. Dashed lines are the predictions using the rate equation. Data from quantum-trajectory simulations for $L = 14$ (symbols) are presented for two times.

the distribution shown in Fig. 2 (right). Starting from a flat distribution at $t = 0$, the distribution displays two peaks centered around $k = \pm\pi/2$ that persist until the mean density reaches $\bar{n} = 0.5$ ($t \leqslant 0.25\Gamma_{\mathrm{eff}}^{-1}$). For lower mean densities ($t > 0.25\Gamma_{\mathrm{eff}}^{-1}$), peaks appear around $k = 0, \pi$, as in the fermionic case. We compare the results of the rate equations with the exact curves obtained with quantum trajectories for $L = 14$. The agreement is excellent at long times and satisfactory at intermediate times $\sim 0.25\Gamma_{\mathrm{eff}}^{-1}$. For very short times $t < 0.1\Gamma_{\mathrm{eff}}^{-1}$ the rate equation reproduces poorly the exact data. The numerical calculations show sizable off-diagonal momentum correlations $\langle c_k^\dagger c_{k'} \rangle$ [51], implying the failure of the prethermalization assumption.

Time-dependent GGE. The theory presented so far can be reformulated using the recently introduced notion of time-dependent GGE (tGGE) [42,43,53–55]. The interest of this reformulation is conceptual: as originally pointed out in Ref. [4], a system in the quantum Zeno regime features quasistationary subspaces and the dynamics constrained therein is generically ruled by a master equation with a strong unitary part and a weak dissipation—as we are considering here. A tGGE establishes a more suitable starting point for the modelization of other experimental setups [33–36].

We rewrite the master equation $\frac{d}{dt}\rho = \mathcal{L}'[\rho]$ as $\frac{d}{dt}\rho = \mathcal{L}_0[\rho] + \mathcal{L}_1[\rho]$. Here $\mathcal{L}_0[\rho] = -\frac{i}{\hbar}[H', \rho]$ describes the dominant unitary dynamics ($\mathcal{L}_0 \propto J/\hbar$), and $\mathcal{L}_1$ the weaker dissipative part ($\mathcal{L}_1 \propto \Gamma_{\mathrm{eff}}$). To lowest order in $\hbar\Gamma_{\mathrm{eff}}/J \ll 1$, the tGGE theory predicts that the system remains at all times in one of the many stationary states of $\mathcal{L}_0$. The effect of the dissipation $\mathcal{L}_1$ is then to determine the dynamics within this subspace.

The tGGE theory relies on a particular *ansatz* for the density matrix. Instead of *all* possible stationary states, the *ansatz* retains only the GGEs for the strong Hamiltonian H',

$$\rho_{\mathrm{tGGE}}(t) = \frac{1}{\mathcal{Z}(t)} e^{-\sum_k \mu_k(t) c_k^\dagger c_k}, \qquad (7)$$

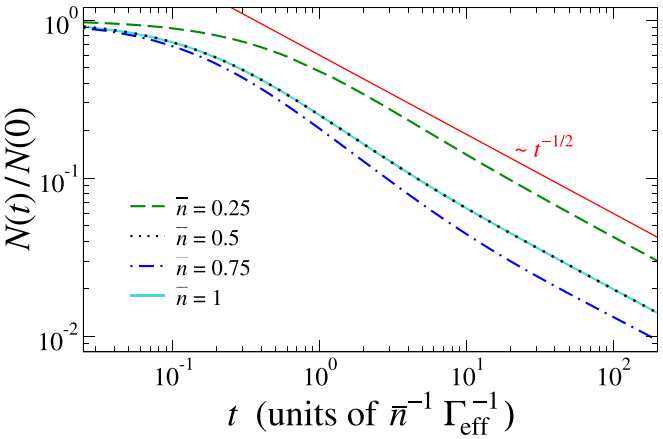

FIG. 3. Decay of atom number for lattice Tonks-Girardeau gases with density $\bar{n} \leqslant 1$. The various curves are calculated according to the rate equations (5) for different initial conditions. The initial state is taken to be a lattice Tonks-Girardeau gas with $n_k(t=0)$ given by the Fermi-Dirac distribution at zero temperature with mean density $\bar{n}$.

with time-dependent Lagrange multipliers $\mu_k(t)$ and a generalized partition function $\mathcal{Z}(t) = \prod_k [1 + e^{-\mu_k(t)}]$. The equations of motion for the $\mu_k(t)$ derived in Ref. [42] describe how $\mathcal{L}_1$ forces the system to explore different GGE states. In our case, we obtain [51]

$$\frac{d}{dt}\mu_k(t) = \frac{4\Gamma_{\rm eff}}{L}\sum_q [\sin(k) - \sin(q)]^2 \frac{e^{-\mu_k(t)}+1}{e^{\mu_q(t)}+1}. \qquad (8)$$

The individual occupation numbers for the state (7) obey a Fermi-Dirac law $n_k(t) = (e^{\mu_k(t)}+1)^{-1}$. Substituting this expression in Eq. (8), we recover the rate equations (5) for $n_k(t)$, thereby establishing the equivalence of the two formulations.

Initial state. The behavior discussed so far is not specific to a Mott insulator initial state with density $\bar{n} = 1$, but is also observed for lower initial fillings. Let us first consider a bosonic gas with equally populated momenta $\langle b_k^\dagger b_k\rangle = \bar{n} < 1$, which maps to $n_k(0) = \bar{n}$. The rate equations can be solved with a proper rescaling of time $t \to t\bar{n}$, so that $n_k(t) = \bar{n} f_k(\bar{n}\Gamma_{\rm eff} t)$. Thus, for a lower initial density, the loss dynamics simply slows down and the effective decay rate is rescaled by the density.

To model a situation closer to experimental reality, we now consider an initial state that is the ground state of the Hamiltonian H' with density $\bar{n} < 1$ (a Tonks-Girardeau gas on a lattice [56]). In the fermionic formulation, the initial conditions are determined by Fermi-Dirac statistics $n_k(0) = n_{\rm FD}(k) = (e^{\beta(-2J\cos k - \mu)}+1)^{-1}$ with $\beta \to +\infty$. The numerical analysis presented in Fig. 3 shows the results of the rate equation with a rescaling $t \to t\bar{n}$. We observe that $\bar{n} = 0.5$ and $\bar{n} = 1$ collapse exactly whereas for $\bar{n} < 0.5$ the dynamics slows down. On the contrary, for values $0.5 < \bar{n} < 1$ the dynamics is slightly faster and nonmonotonic in the density. Thus, the decay can be accelerated or decelerated depending on the initial density. In all cases, however, we observe a long-time decay $N(t) \sim t^{-1/2}$. This robust feature of a slower decay thus remains the strongest evidence for the interplay between correlations and losses beyond the mean-field description.

Conclusions and perspectives. We have proposed a theoretical approach to the dynamics of a lossy bosonic gas in the many-body quantum Zeno regime. The quasistationary subspace enables a theoretical treatment based on generalized thermalization.

From an experimental viewpoint, the discussed dynamics can be investigated with any atomic or molecular species featuring strong two-body losses [17,30,33–35], or possibly in other systems as well (for instance, photonic systems with two-photon absorption [10]). We can estimate the relevant timescales for an optical lattice of 8 recoil energies ($U/J \sim 20$) loaded with ^{174}Yb in its metastable excited state (on-site two-body losses have been characterized in Refs. [57,58]). We obtain $U/\hbar = 7800\ \mathrm{s}^{-1}$, $\gamma_{2B} = 5900\ \mathrm{s}^{-1}$, and $J/\hbar = 377\ \mathrm{s}^{-1}$ and as a result $\Gamma_{\rm eff} = 24\ \mathrm{s}^{-1}$. Thus, our predictions require an observation time of $20\Gamma_{\rm eff}^{-1} \sim 1$ s which is within current experimental possibilities, although at such timescales there are several difficulties to overcome, such as the fact that the system will almost be depopulated, or that decoherence sources typically ignored could start to play a role.

Since the conservation of the momentum occupation numbers in-between loss events plays a crucial role, an experimental difficulty is the realization of a truly homogeneous system. Although this has been already achieved experimentally [59], the vast majority of experiments also include an additional harmonic confinement [60]. Adapting the rate equation approach to inhomogeneous, harmonically confined systems is an important extension left for future work. Another avenue comes from the tGGE formulation of the dynamics. This establishes a suitable starting point to describe, e.g., fermions with two-body losses [33–35] or bosons with three-body losses [36] and to explore two- and three-dimensional systems.

Note added in proof. While completing this Letter, we became aware of a work discussing losses in one-dimensional bosonic gases without lattice [61].

Acknowledgments. We are grateful to J. De Nardis for discussions on the bosonic momentum distribution function and to I. Bouchoule for insightful comments. We also acknowledge discussions with A. De Luca, M. Fagotti, R. Fazio, G. La Rocca, L. Rosso, and M. Schirò. D.R. acknowledges hospitality from LPTMS through CNRS funding. This work has been partially funded by LabEx PALM (ANR-10-LABX-0039-PALM).

[1] W. H. Zurek, Rev. Mod. Phys. **75**, 715 (2003).
[2] B. Misra and E. C. G. Sudarshan, J. Math. Phys. **18**, 756 (1977).
[3] W. M. Itano, D. J. Heinzen, J. J. Bollinger, and D. J. Wineland, Phys. Rev. A **41**, 2295 (1990).
[4] P. Facchi and S. Pascazio, Phys. Rev. Lett. **89**, 080401 (2002).
[5] A. Beige, D. Braun, and P. L. Knight, New J. Phys. **2**, 22 (2000).
[6] A. Beige, D. Braun, B. Tregenna, and P. L. Knight, Phys. Rev. Lett. **85**, 1762 (2000).

[7] J. Kempe, D. Bacon, D. A. Lidar, and K. B. Whaley, Phys. Rev. A **63**, 042307 (2001).

[8] J. T. Barreiro, M. Müller, P. Schindler, D. Nigg, T. Monz, M. Chwalla, M. Hennrich, C. F. Roos, P. Zoller, and R. Blatt, Nature (London) **470**, 486 (2011).

[9] T. Boulier, M. J. Jacquet, A. Maître, G. Lerario, F. Claude, S. Pigeon, Q. Glorieux, A. Amo, J. Bloch, A. Bramati, and E. Giacobino, Adv. Quantum Technol. **3**, 2000052 (2020).

[10] I. Carusotto, A. A. Houck, A. J. Kollár, P. Roushan, D. I. Schuster, and J. Simon, Nat. Phys. **16**, 268 (2020).

[11] J. Söding, D. Guéry-Odelin, P. Desbiolles, F. Chevy, H. Inamori, and J. Dalibard, Appl. Phys. B **69**, 257 (1999).

[12] B. Laburthe Tolra, K. M. O'Hara, J. H. Huckans, W. D. Phillips, S. L. Rolston, and J. V. Porto, Phys. Rev. Lett. **92**, 190401 (2004).

[13] E. Haller, M. Rabie, M. J. Mark, J. G. Danzl, R. Hart, K. Lauber, G. Pupillo, and H.-C. Nägerl, Phys. Rev. Lett. **107**, 230404 (2011).

[14] T. F. Schmidutz, I. Gotlibovych, A. L. Gaunt, R. P. Smith, N. Navon, and Z. Hadzibabic, Phys. Rev. Lett. **112**, 040403 (2014).

[15] R. Labouvie, B. Santra, S. Heun, and H. Ott, Phys. Rev. Lett. **116**, 235302 (2016).

[16] B. Rauer, P. Grišins, I. E. Mazets, T. Schweigler, W. Rohringer, R. Geiger, T. Langen, and J. Schmiedmayer, Phys. Rev. Lett. **116**, 030402 (2016).

[17] T. Tomita, S. Nakajima, I. Danshita, Y. Takasu, and Y. Takahashi, Sci. Adv. **3**, e1701513 (2017).

[18] R. Bouganne, M. Bosch Aguilera, A. Ghermanoui, J. Beugnon, and F. Gerbier, Nat. Phys. **16**, 21 (2019).

[19] I. Bouchoule and M. Schemmer, SciPost Phys. **8**, 60 (2020).

[20] F. Verstraete, M. M. Wolf, and J. I. Cirac, Nat. Phys. **5**, 633 (2009).

[21] S. Diehl, A. Micheli, A. Kantian, B. Kraus, H.-P. Büchler, and P. Zoller, Nat. Phys. **4**, 878 (2008).

[22] M. Roncaglia, M. Rizzi, and J. I. Cirac, Phys. Rev. Lett. **104**, 096803 (2010).

[23] Z. Gong, S. Higashikawa, and M. Ueda, Phys. Rev. Lett. **118**, 200401 (2017).

[24] M. Schemmer and I. Bouchoule, Phys. Rev. Lett. **121**, 200401 (2018).

[25] L. H. Dogra, J. A. P. Glidden, T. A. Hilker, C. Eigen, E. A. Cornell, R. P. Smith, and Z. Hadzibabic, Phys. Rev. Lett. **123**, 020405 (2019).

[26] Y. Ashida, Z. Gong, and M. Ueda, Adv. Phys. **69**, 249 (2021).

[27] A. J. Daley, J. M. Taylor, S. Diehl, M. Baranov, and P. Zoller, Phys. Rev. Lett. **102**, 040402 (2009).

[28] A. Kantian, M. Dalmonte, S. Diehl, W. Hofstetter, P. Zoller, and A. J. Daley, Phys. Rev. Lett. **103**, 240401 (2009).

[29] M. Foss-Feig, A. J. Daley, J. K. Thompson, and A. M. Rey, Phys. Rev. Lett. **109**, 230501 (2012).

[30] N. Syassen, D. M. Bauer, M. Lettner, T. Volz, D. Dietze, J. J. García-Ripoll, J. I. Cirac, G. Rempe, and S. Dürr, Science **320**, 1329 (2008).

[31] J. J. García-Ripoll, S. Dürr, N. Syassen, D. M. Bauer, M. Lettner, G. Rempe, and J. I. Cirac, New J. Phys. **11**, 013053 (2009).

[32] T. Tomita, S. Nakajima, Y. Takasu, and Y. Takahashi, Phys. Rev. A **99**, 031601(R) (2019).

[33] B. Yan, S. A. Moses, B. Gadway, J. Covey, K. R. A. Hazzard, A. M. Rey, D. S. Jin, and J. Ye, Nature (London) **501**, 521 (2013).

[34] B. Zhu, B. Gadway, M. Foss-Feig, J. Schachenmayer, M. L. Wall, K. R. A. Hazzard, B. Yan, S. A. Moses, J. P. Covey, D. S. Jin, J. Ye, M. Holland, and A. M. Rey, Phys. Rev. Lett. **112**, 070404 (2014).

[35] K. Sponselee, L. Freystatzky, B. Abeln, M. Diem, B. Hundt, A. Kochanke, T. Ponath, B. Santra, L. Mathey, K. Sengstock, and C. Becker, Quantum Sci. Technol. **4**, 014002 (2019).

[36] M. J. Mark, S. Flannigan, F. Meinert, J. P. D'Incao, A. J. Daley, and H.-C. Nägerl, Phys. Rev. Research **2**, 043050 (2020).

[37] T. Langen, S. Erne, R. Geiger, B. Rauer, T. Schweigler, M. Kuhnert, W. Rohringer, I. E. Mazets, T. Gasenzer, and J. Schmiedmayer, Science **348**, 207 (2015).

[38] F. H. L. Essler and M. Fagotti, J. Stat. Mech. (2016) 064002.

[39] M. A. Cazalilla and M.-C. Chung, J. Stat. Mech. (2016) 064004.

[40] L. Vidmar and M. Rigol, J. Stat. Mech. (2016) 064007.

[41] T. Langen, T. Gasenzer, and J. Schmiedmayer, J. Stat. Mech. (2016) 064009.

[42] F. Lange, Z. Lenarčič, and A. Rosch, Phys. Rev. B **97**, 165138 (2018).

[43] K. Mallayya, M. Rigol, and W. De Roeck, Phys. Rev. X **9**, 021027 (2019).

[44] J.-S. Caux, B. Doyon, J. Dubail, R. Konik, and T. Yoshimura, SciPost Phys. **6**, 70 (2019).

[45] M. Schemmer, I. Bouchoule, B. Doyon, and J. Dubail, Phys. Rev. Lett. **122**, 090601 (2019).

[46] S. Goto and I. Danshita, Phys. Rev. A **102**, 033316 (2020).

[47] For $J = 0$, the population of doubly-occupied sites decays as $p_2(t) = p_2(0)e^{-\gamma_{2B}t}$.

[48] A. J. Daley, Adv. Phys. **63**, 77 (2014).

[49] P. Jordan and E. P. Wigner, Z. Phys. **47**, 631 (1928).

[50] S. Sotiriadis and P. Calabrese, J. Stat. Mech. (2014) P07024.

[51] See Supplemental Material at http://link.aps.org/supplemental/10.1103/PhysRevA.103.L060201 for contains information on (I) the derivation of the rate equation, (II) the long-time behaviour of the rate equation, (III) the momentum distribution functions, (IV) the time-dependent generalised Gibbs ensemble.

[52] D. M. Gangardt and G. V. Shlyapnikov, New J. Phys. **8**, 167 (2006).

[53] F. Lange, Z. Lenarčič, and A. Rosch, Nat. Commun. **8**, 15767 (2017).

[54] Z. Lenarčič, F. Lange, and A. Rosch, Phys. Rev. B **97**, 024302 (2018).

[55] F. Reiter, F. Lange, S. Jain, M. Grau, J. P. Home, and Z. Lenarčič, arXiv:1910.01593.

[56] M. Girardeau, J. Math. Phys. **1**, 516 (1960).

[57] R. Bouganne, M. B. Aguilera, A. Dareau, E. Soave, J. Beugnon, and F. Gerbier, New J. Phys. **19**, 113006 (2017).

[58] L. Franchi, L. F. Livi, G. Cappellini, G. Binella, M. Inguscio, J. Catani, and L. Fallani, New J. Phys. **19**, 103037 (2017).

[59] A. Mazurenko, C. S. Chiu, G. Ji, M. F. Parsons, M. Kanász-Nagy, R. Schmidt, F. Grusdt, E. Demler, D. Greif, and M. Greiner, Nature **545**, 462 (2017).

[60] I. Bloch, J. Dalibard, and W. Zwerger, Rev. Mod. Phys. **80**, 885 (2008).

[61] I. Bouchoule, B. Doyon, and J. Dubail, SciPost Phys. **9**, 44 (2020).